Optics Letters

Electro-optical effects of high aspect ratio P3HT nanofibers colloid in polymer micro-fluid cells

G. S. Lobov,[1,*] A. Marinins,[1] R. Zandi Shafagh,[2] Y. Zhao,[1] W. van der Wijngaart,[2] L. Wosinski,[1] L. Thylen,[3] M. S. Toprak,[1] T. Haraldsson,[2] M. Östling,[4] and S. Popov[1]

[1]School of Engineering Sciences, KTH Royal Institute of Technology, Stockholm SE10691, Sweden
[2]Micro and Nanosystems, KTH Royal Institute of Technology, Stockholm SE10044, Sweden
[3]School of Biotechnology, KTH Royal Institute of Technology, Stockholm SE10691, Sweden
[4]School of Information and Communication Technology, KTH Royal Institute of Technology, Stockholm 16440, Sweden
*Corresponding author: lobov@kth.se

Received 5 April 2017; revised 26 April 2017; accepted 10 May 2017; posted 10 May 2017 (Doc. ID 292225); published 30 May 2017

This Letter reports the electro-optical (EO) effect of Poly(3-hexylthiophene-2,5-diyl) (P3HT) nanofibers colloid in a polymer micro-fluidic EO cell. P3HT nanofibers are high aspect ratio semiconducting nanostructures, and can be collectively aligned by an external alternating electric field. Optical transmission modulated by the electric field is a manifestation of the electro-optical effect due to high inner crystallinity of P3HT nanofibers. According to our results, the degree of alignment reaches a maximum at 0.6 V/μm of electric field strength, implying a big polarizability value due to geometry and electrical properties of P3HT nanofibers. We believe that one-dimensional crystalline organic nanostructures have a large potential in EO devices due to their significant anisotropy, wide variety of properties, low actuation voltages, and opportunity to be tailored via adjustment of the fabrication process.

OCIS codes: (160.5470) Polymers; (160.2100) Electro-optical materials; (160.1190) Anisotropic optical materials; (140.3948) Microcavity devices.

https://doi.org/10.1364/OL.42.002157

Anisotropic one-dimensional (1D) nanostructures, such as metallic nanorods, carbon nanotubes, and organic nanofibers, have been proven suitable for a variety of nanoelectronic and photonic applications [1,2]. Organic 1D nanostructures with a high crystallinity possess a wide range of unique optical properties, such as dichroic absorption [3], birefringence [4], and polarized photoluminescence [5]. The ability to control the alignment of dispersed 1D nanostructures by an electric field makes them especially promising for electro-optical (EO) devices. Currently, the field of EO materials focuses largely on liquid crystals (LC) and dichroic dyes [6]. Unlike LC, synthetic 1D nanostructures do not require surface alignment layers and are easily tunable in size and properties [7]. Hence, colloids of organic 1D nanostructures can function as dye-doped liquid crystals, which in combination with high chemical stability and strong EO response may be implemented in applications such as displays and optical switches among others.

The characterization of 1D nanostructure colloids plays an important role in developing a material with required properties. This is done by encapsulating the colloid in an EO cell, allowing the properties of light to be monitored, transmitted through the suspension, while tuning the external electric field [8]. EO cells typically consist of two spatially separated coated glass substrates (longitudinal EO cell) [6,9,10], inconvenient for studying liquids, or of sophisticated optofluidic waveguides (transverse EO cell) [11].

In this work we have studied the EO response of Poly(3-hexylthiophene-2,5-diyl) (P3HT) nanofibers, by controlling their alignment in a longitudinal EO cell. We fabricated the cell using reaction injection molding (RIM) of the ultraviolet (UV) sensitive off-stoichiometric thiol–ene epoxy (OSTE+) polymer [12,13], followed by area selective Teflon AF coating and covalent bonding of the two parts using the remaining native bonding areas. The microfluidic cell was designed to feature a small cavity volume (~250 μl), a spacing of 175 μm between the electrodes, hermetic sealing, and tolerance against organic solvents. We confirmed that the dynamic reorientation of P3HT nanofibers by an external alternating electric field leads to intensity modulation of transmitted 532 nm light. The maximum ordering of nanofibers was reached at 0.64 V/μm. We attribute such strong electrical response to a large polarizability of P3HT nanofibers, due to their high aspect ratio (~75) and high carrier mobility, and the presence of an extra positive charge. For comparison, gold nanorods with aspect ratio of 2.5 require >1 V/um [9]. Semiconducting CdSe nanorods with aspect ratio of 10 can be completely aligned at ~15 V/μm [10], while some liquid crystals require >0.7 V/μm for full alignment [14].

Off-stoichiometric thiol–ene epoxy (OSTE+) polymer (OSTEMER 322, Mercene Labs AB, Sweden) was chosen as the polymer cell material because of high optical transparency, ability to be rapidly UV cured, and presence of epoxy and thiol groups on the surface, allowing direct epoxy bonding

OSTE+ layers and gold deposition with covalent bonding of gold to thiol groups. During the fabrication process complementary parts of the component (Fig. 1) were made by RIM of OSTE+ polymer precursor using aluminum molds and UV curing. After the polymerization process, semitransparent layers of 20 nm thick gold were deposited (Fig. 1) to form the electrodes. A thin passivation layer of Teflon was spin coated on selected areas to prevent warping of the cavity by solvent swelling of the OSTE+. Finally, the two polymer parts were assembled together and cured in an oven at 120°C for 30 min to obtain a stiff monolithic device. After this second curing step, the polymer was fully cured resulting in a solid material with inert hydroxyl groups on the surface.

The exposed areas of the gold electrodes were connected to the signal source by glued wires. The signal source consisted of a wavegenerator, a pulse generator, and a single-pole double-throw (SPDT) switch. The wavegenerator supplied a sine wave signal, with tunable frequency and amplitude. The pulse generator and the SPDT switch modulated the continuous sinewave from the wavegenerator into intermittent pulses of sinewave of a desired duration (Fig. 2). The EO cell was placed into the setup such that the gold electrodes were perpendicular to the 532 nm laser diode beam. The colloid with P3HT nanofibers was injected into the cavity via tubing connected to the inlet and outlet ports of the cell. The intensity of the transmitted light was recorded by the detector. The overall transmission of the EO cell with nanofibers colloid was approximately 0.09 and was to a major extent defined by the transmission of semitransparent gold layers.

P3HT nanofibers are high aspect ratio p-type semiconducting structures, formed by ordered stacking of P3HT molecules [15]. P3HT nanofibers dispersed in anisole are positively charged, wherein the positive charge can travel along the nanofiber length by hopping [3]. The presence of a positive charge is attributed to the oxidation reaction with anisole [15], and plays

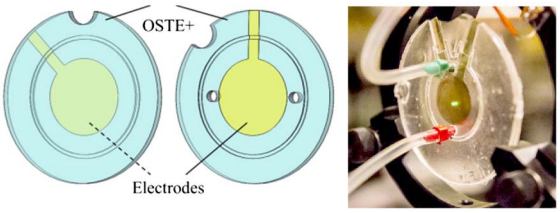

Fig. 1. Design of the optofluidic component.

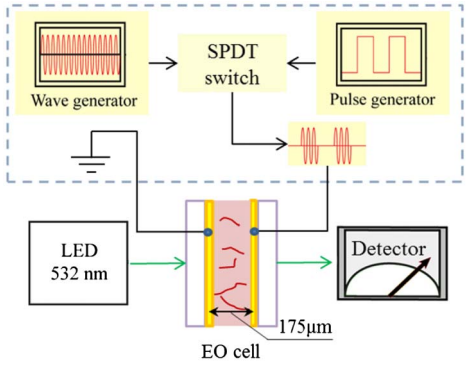

Fig. 2. Schematic layout of the measurement setup.

an important role in the colloid stability and polarizability. In our experiments P3HT nanofibers with an average length of 1–1.5 μm and width of ~20 nm were produced by the mixed solvent method, allowing nanofibers of various length to be grown [16]. During fabrication, 10 mg of commercially available P3HT (Luminescence Technology Corporation, Taiwan, China) were mixed with 5 ml of anisole (Sigma Aldrich) and sonicated for 10 min. After that 5 ml of chloroform was added, after which the solution was sonicated for 10 min and placed in a dark environment for 72 h under a continuous nitrogen flow. Finally, the colloid was diluted with anisole to a desired density of $4.36 \cdot 10^8 \pm 3\%$ units/μl, where the final value was defined empirically based on the balance between the appropriate light transmission and electro-optical response.

When dispersed P3HT nanofibers are placed into an alternating electric field of frequency much lower than optical, and the redistribution of positive charges along the long axis leads to formation of induced dipole μ and rotation torque M, aligning the nanofibers along the electric field lines. The polarizability γ of the particles with mobile charges is defined in the low-frequency limit by the conductivities of the particle and the media, and is proportional to the particle volume [17–19].

An EO effect in colloids can be expressed through the parameter N, in terms of its saturated value N^{sat} and the particle orientation function $\Phi(E, t)$ as follows [18,19]:

$$N = N^{\text{sat}} \cdot \Phi(E). \tag{1}$$

The particle orientation function for induced dipoles in weak alternating electric field of shape $E \cdot \sin(\omega t)$ has the form as in Eq. (2),

$$\Phi(E) = \frac{\gamma E^2}{15\ \text{kT}}, \tag{2}$$

where $\gamma = \gamma_{\parallel} - \gamma_{\perp}$, with $\gamma_{\parallel}$ and $\gamma_{\perp}$ - polarizabilities of the nanofibers along and perpendicular to the main axis, respectively, and E is the effective value. For the case of the strong electric field Eq. (3) should be used, as follows:

$$\Phi(E) = 1 - \frac{3}{\frac{\gamma E^2}{\text{kT}} - 1}. \tag{3}$$

From previous observations it is known that P3HT nanofibers possess such optical properties as dichroic absorption (in spectral range 450–600 nm) and optical birefringence (650–1550 nm) [20]. The light with polarization perpendicular to the nanofibers' long axis is absorbed stronger than light with the parallel polarization. The fast optical axis of nanofibers is oriented perpendicular to their long axis, i.e., parallel to the chain axis. These properties may be attributed to dichroic conductivity of nanofibers, resulting from their structural crystallinity. The mobility of charges along the nanofibers' long axis is defined by a hopping mechanism and is lower than the mobility along the chain axis of P3HT molecules, while the mobility along the side chains is negligible [15].

When an alternating electric field is applied to the electrodes, nanofibers are aligned along the light beam and perpendicularly to the polarization vector of incident light, and, therefore, to the transmission signal decays. After the electric field is switched off, P3HT nanofibers thermally relax to a disordered state. As in the disordered state nanofibers do not form domains or aggregates, and the initial polarization of the incident light is regained. Moreover, since no surface alignment of the EO cell walls is involved, the effect is polarization independent. If the wavelength

of the laser source is within the range of 650–1550 nm, the abovementioned approach can be used for modulation of the optical phase with no changes in output intensity.

The response time was defined as the time needed for the transmission signal to reach 80% of the maximum decay. The amplitude of transmission modulation was calculated using Eq. (4),

$$\frac{\Delta T}{T_0} = \frac{T_0 - T}{T_0}, \tag{4}$$

where T_0 is the initial transmission level, and T is the transmission level after the time delay equal to the response time. The transmission modulation and response time with respect to the amplitude of the applied electric field are shown in Figs. 3(a) and 3(b), respectively. The modulation amplitude is saturated at approximately 0.6 V/μm, while the response time continues to decay with the increasing electric field down to 10 ms at 1.7 V/μm. The experimental data in Fig. 3(a) was fitted with Eq. (1), whereas the $\Phi(E)$ function was a piecewise function, consisting of Eqs. (2) and (3) with a stitching parameter, which was also fitted. The results of the fitting correspond to $N^{\text{sat}} = 0.1351$, $\gamma = 1 \cdot 10^{-10}$ kT, and stitching parameter of 0.45 V/μm.

The dependence of transmission modulation and response time on the frequency of the applied electric field is shown in Figs. 4(a) and 4(b), respectively. The response of P3HT nanofibers decreases for frequencies above 3 kHz, of which can be explained by the limited mobility of charges [21]. At higher frequencies the displacement of charges becomes less pronounced and the rotary torque, which aligns nanofibers, becomes weaker. As the result, the thermal fluctuations introduce more randomness to the system, affecting the degree of orientation and, thus, the transmission modulation.

An oscillatory component of the modulated transmission signal was observed at low frequencies [22], as nanofibers had enough time to relax while the polarity of the alternating electric field was changing. The oscillatory component became smaller and smaller with rising frequency and disappeared at a cutoff frequency of 1.5 kHz. The diffusion coefficient D can be approximately calculated knowing the cutoff frequency f_r of the oscillatory component as follows [22]:

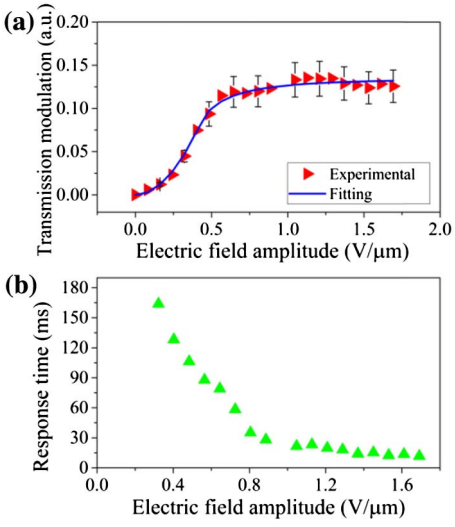

Fig. 3. Transmission modulation (a) and response time (b) versus the amplitude of applied sinewave electric field with frequency 2 kHz.

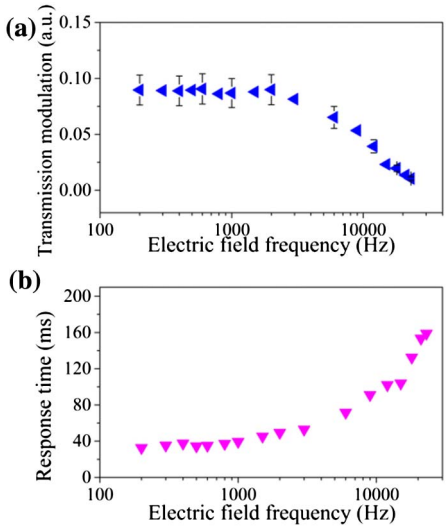

Fig. 4. Transmission modulation (a) and response time (b) versus the frequency of applied sinewave electric field with amplitude 0.8 V/μm.

$$D = \frac{f_r}{6} = 2.5 \cdot 10^2 \ \frac{1}{\text{s}}. \tag{5}$$

The amplitude of transmission modulation of the signal with an oscillatory component was calculated using values of the local minima of oscillations as the value of T [Eq. (4)].

In summary, we demonstrated a facile and cost-effective technique for fabricating a polymer microfluidic EO cell using the OSTE+ RIM platform. The previously demonstrated capability of such a technique for polymer submicron structuring down to 250 nm [23] acts as an enabler for easy downscaling of feature sizes for future demands.

We have also performed the EO characterization of 1–1.5 μm long conductive P3HT nanofibers dispersed in a nonconductive media. The degree of alignment is saturated at approximately 0.6 V/μm. The mechanism of polarizability is attributed to mobile charges in P3HT nanofibers, which are dispersed in nonconductive media. In such a case, the polarizability of P3HT nanofibers depends linearly on their volume, providing an opportunity to tune the responsivity by adjusting nanofiber length.

Funding. Seventh Framework Programme (FP7) EU project ICON (608099); Vetenskapsrådet (VR) (VR-SRL 2012-4421, VR-SRL 2013-6780); Stiftelsen för Strategisk Forskning (SSF) (EM11-0002).

Acknowledgment. The authors acknowledge Dr. Abhilash Sugunan from SP Technical Research Institute of Sweden for insightful discussions regarding the material properties and fabrication. We also express our gratitude to Mercene Lab for providing the OSTEMER polymer and to Dr. Sergey Dyakov from Skolkovo Institute of Science and Technology for experimental data analysis.

REFERENCES

1. O. Stamatoiu, J. Mirzaei, X. Feng, and T. Hegmann, Top. Curr. Chem. **318**, 331 (2011).
2. S. Moynihan, P. Lovera, D. O'Carroll, D. Iacopino, and G. Redmond, Adv. Mater. **20**, 2497 (2008).

3. G. S. Lobov, Y. Zhao, A. Marinins, M. Yan, J. Li, M. S. Toprak, A. Sugunan, L. Thylen, L. Wosinski, M. Östling, and S. Popov, Opt. Mater. Express **5**, 2642 (2015).
4. G. S. Lobov, Y. Zhao, A. Marinins, M. Yan, J. Li, M. S. Toprak, A. Sugunan, L. Thylen, L. Wosinski, M. Östling, and S. Popov, Macromol. Chem. Phys. **217**, 1089 (2016).
5. K. Yin, L. Zhang, C. Lai, L. Zhong, S. Smith, H. Fong, and Z. Zhu, J. Mater. Chem. **21**, 444 (2011).
6. J. Fontana, G. K. B. da Costa, J. M. Pereira, J. Naciri, B. R. Ratna, P. Palffy-Muhoray, and I. C. S. Carvalho, Appl. Phys. Lett. **108**, 081904 (2016).
7. A. de la Cotte, P. Merzea, J. W. Kim, K. Lahlil, J.-P. Boilot, T. Gacoin, and E. Grelet, Soft Matter **11**, 6595 (2015).
8. H. Yu, D. Y. Kim, K. J. Lee, and J. H. Oh, J. Nanosci. Nanotechnol. **14**, 1282 (2014).
9. P. Zijlstra, M. V. Stee, N. Verhart, Z. Gu, and M. Orrit, Phys. Chem. Chem. Phys. **14**, 4584 (2012).
10. M. Mohammadimasoudi, Z. Hens, and K. Neyts, RSC Adv. **6**, 55736 (2016).
11. X. He, Q. Shao, P. Cao, W. Kong, J. Sun, X. Zhang, and Y. Deng, Lab Chip **15**, 1311 (2015).
12. N. Sandström, R. Z. Shafagh, A. Vastesson, C. F. Carlborg, W. van der Wijngaart, and T. Haraldsson, J. Micromech. Microeng. **25**, 075002 (2015).
13. C. F. Carlborg, A. Vastesson, Y. Liu, W. van der Wijngaart, M. Johansson, and T. Haraldsson, J. Polym. Sci. A **52**, 2604 (2014).
14. Y.-H. Lin, H. Ren, Y.-H. Wu, Y. Zhao, J. Fang, Z. Ge, and S.-T. Wu, Opt. Express **13**, 8746 (2005).
15. K. Tremel and S. Ludwigs, Adv. Polym. Sci. **265**, 39 (2014).
16. Y. Zhao, A. Sugunan, D. B. Rihtnesberg, Q. Wang, M. S. Toprak, and M. Muhammed, Phys. Status Solidi C **9**, 1546 (2012).
17. S. A. Klemeshev, M. P. Petrov, A. K. Shalygin, A. A. Trusov, A. V. Voitylov, and V. V. Vojtylov, Colloids Surf. A **456**, 114 (2014).
18. S. A. Klemeshev, M. P. Petrov, A. A. Trusov, and A. V. Voitylov, J. Phys. Condens. Matter **22**, 494106 (2010).
19. S. P. Stoylov and M. V. Stoimenova, *Molecular and Colloidal Electrooptics* (CRC Press, 2006).
20. G. S. Lobov, Y. Zhao, A. Marinins, M. Yan, J. Li, M. S. Toprak, A. Sugunan, L. Thylen, L. Wosinski, M. Östling, and S. Popov, Adv. Opt. Mater. **4**, 1651 (2016).
21. T. Prodromakis and C. Papavassiliou, Appl. Surf. Sci. **255**, 6989 (2009).
22. A. V. Delgadoa, F. Carriqueb, F. J. Arroyoa, T. Bellinic, F. Mantegazzac, M. E. Giardinic, and V. Degiorgioc, Colloids Surf. A **140**, 157 (1998).
23. R. Z. Shafagh, W. van der Wijngaart, and T. Haraldsson, *Proceedings of the 30th IEEE International Conference on Micro Electro Mechanical Systems* (2017).